Journal of the Geological Society, London, Vol. **163**, 2006, pp. 375–382. Printed in Great Britain.

Upper Cretaceous carbon- and oxygen-isotope stratigraphy of hemipelagic carbonate facies from southern Tibet, China

XIANGHUI LI[1], HUGH C. JENKYNS[2], CHENGSHAN WANG[3], XIUMIAN HU[4], XI CHEN[1], YUSHUAI WEI[1], YONGJIAN HUANG[1] & JIE CUI[1]

[1]*State Key Laboratory of Oil & Gas Reservoir Geology and Exploitation, Chengdu University of Technology, Chengdu, P.R. China (e-mail: lixh@cdut.edu.cn)*

[2]*Department of Earth Sciences, University of Oxford, Oxford OX1 3PR, UK*

[3]*China University of Geosciences, Beijing, P.R. China*

[4]*Department of Earth Sciences, Nanjing University, Nanjing, P.R. China*

Abstract: A high-resolution carbon-isotope curve derived from Upper Cretaceous hemipelagic sediments cropping out at Tingri, southern Tibet, shows similarities to patterns established on other continents, notably in the presence of a well-defined positive excursion across the Cenomanian–Turonian boundary where $\delta^{13}C$ values exceed 3.5‰. From the upper Turonian to the lower Campanian, $\delta^{13}C$ values generally decline, apart from a minor positive excursion in the middle Coniacian: a trend that departs from that recorded from Europe. Relatively low $\delta^{13}C$ values (*c*. 1‰) at the Santonian–Campanian and Campanian–Maastrichtian boundaries in Tibet define a prominent broad positive excursion centred in the middle Campanian and terminated by an abrupt fall towards the close of the stage. When compared with data from Europe and North Africa, the $\delta^{13}C$ values of the Tibetan section are generally lower by *c*. 1.5‰, except for the middle Campanian positive excursion where values ($\delta^{13}C$ *c*. 2‰) are comparable with those documented from Europe and North Africa. These differences are interpreted as reflecting variable mixing of water masses carrying different carbon-isotope signatures, such that areas close to the major sinks of marine organic carbon recorded higher $\delta^{13}C$ values than those located in more distal regions. Oxygen-isotope ratios, albeit affected by diagenesis, may record a palaeotemperature signal.

Since the publication of the pioneering paper on Cretaceous carbon-isotope stratigraphy by Scholle & Arthur (1980), numerous carbon-isotope curves illustrating both long-term (Phanerozoic) and short-term (stage duration) trends have been established both as an aid to stratigraphic correlation and as a monitor of changes in the global carbon cycle, sea level and palaeoclimate (e.g. Arthur *et al*. 1987; Schlanger *et al*. 1987; Weissert 1989; Gale *et al*. 1993; Jenkyns *et al*. 1994; Voigt & Hilbrecht 1997; Veizer *et al*. 1999; Stoll & Schrag 2000; Weissert & Erba 2004). The original interpretation of Scholle & Arthur (1980), that positive shifts in the global carbon-isotope curve primarily relate to increased global burial rates of relatively isotopically light organic carbon in black shales, particularly during Oceanic Anoxic Events, has remained current (e.g. Schlanger & Jenkyns 1976; Jenkyns 1980; Schlanger *et al*. 1987; Arthur *et al*. 1990; Gale *et al*. 1993; Tsikos *et al*. 2004). Large negative excursions (*c*. 2–4‰), particularly if apparently abrupt, imply introduction of isotopically light carbon into the ocean–atmosphere system and have been recently interpreted as related to a flux of methane ($\delta^{13}C$ *c*. −60‰) from dissociation of gas hydrates (e.g. Dickens *et al*. 1995; Jahren *et al*. 2001; Jenkyns 2003). The early studies on Late Cretaceous carbon-isotope trends were undertaken in Europe and North America but curves now also exist for sections in North Africa, South America, the central Pacific, Japan and the Russian Far East, the material analysed including pelagic carbonate, marine and terrestrial organic matter (Boersma & Shackleton 1981; Pratt & Threlkeld 1984; Arthur *et al*. 1988; Jenkyns *et al*. 1995; Hasegawa 1997; Villamil & Arango 1998; Jarvis *et al*. 2002; Hasegawa *et al*. 2003). Latterly, increasingly high-resolution studies have revealed detailed structure in many carbon-isotope curves derived from Upper Cretaceous pelagic carbonates and black shales (e.g. Paul *et al*. 1999; Tsikos *et al*. 2004; Bowman & Bralower 2005; Erbacher *et al*. 2005). Long-term oxygen-isotope profiles, based either on bulk carbonate or single-species Foraminifera, illustrate general climatic decline during the mid- to Late Cretaceous (e.g. Huber *et al*. 1995, 2002; Clarke & Jenkyns 1999; Zakharov *et al*. 1999).

Because of poor accessibility of the key outcrops, comparable isotopic data are, however, relatively sparse for the Tethys Himalayas although continually exposed sections in appropriate pelagic to hemipelagic facies are present (Hu *et al*. 2001; Wang *et al*. 2001; Wan *et al*. 2003*a*, *b*). Here we present a high-resolution carbon- and oxygen-isotope stratigraphy for the Gongzha section, located some 50 km west of Tingri in the southern Tethys Himalayas (Figs 1 and 2).

Stratigraphy and lithofacies

Tectonically, South Tibet is composed of five zones (Fig. 1): High Himalayas; Tethys Himalayas; Yarlung Zangbo suture; Xigaze forearc basin; Gandese Arc (Gansser 1964, 1991). The Tethys Himalayas are further subdivided into a northern and southern unit by an east–west strike-slip fault (Wang *et al*. 1996). Three lithostratigraphic units constitute the Upper Cretaceous succession exposed at Gongzha; these are, in ascending order, the Lengqingre Formation, the Gamba Cunkou Formation and the Zongshan Formation (Fig. 2). In the Tingri area, an initial bio- and chronostratigraphy of the Upper Cretaceous was formulated in the 1980s and 1990s (Hao & Wan 1985; Willems

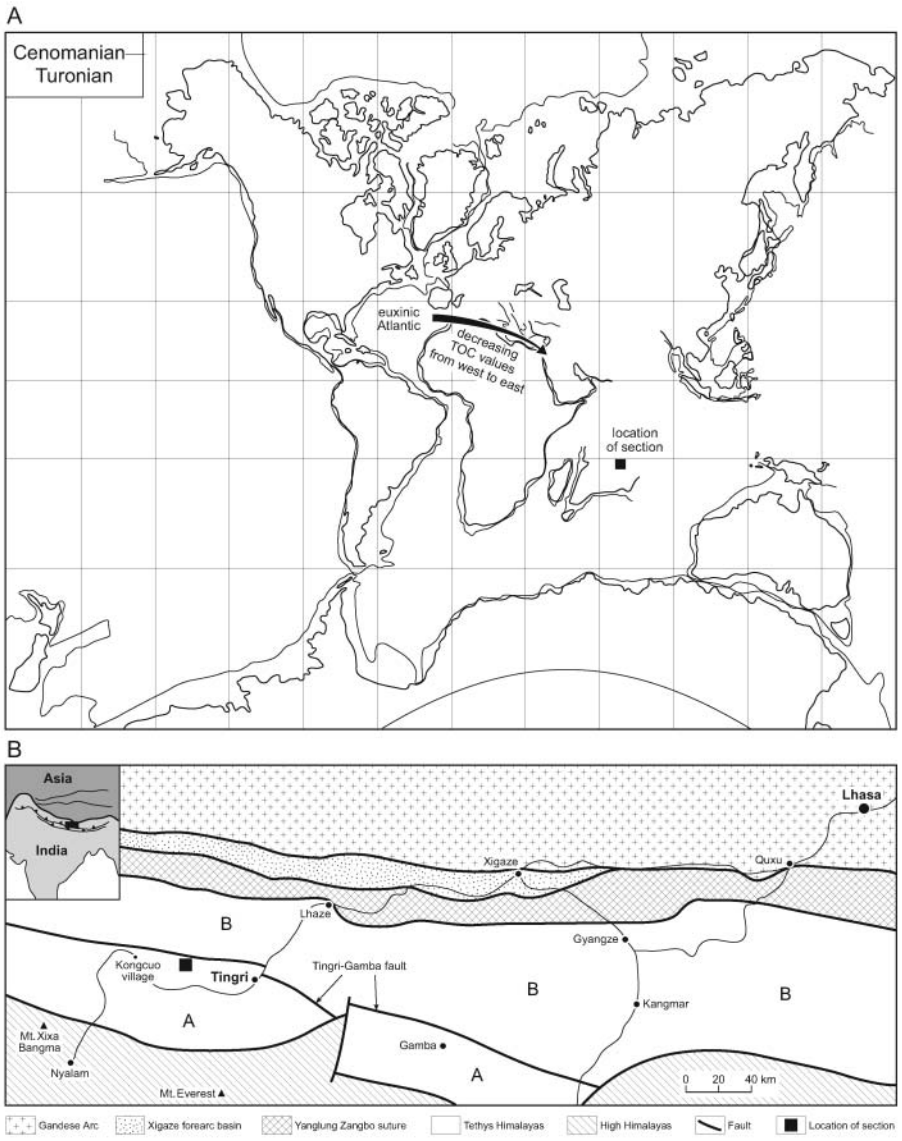

Fig. 1. (**a**) Palaeocontinental reconstruction at Cenomanian–Turonian boundary time, showing the probable location of the investigated section: modified from Smith *et al*. (1981). It should be noted that the degree of organic-carbon enrichment (TOC; total organic carbon) at the Cenomanian–Turonian boundary decreases from west to east in an Atlantic–North African transect (Lüning *et al*. 2004), in accord with the interpretation that the resultant $\delta^{13}C$ signature was progressively diluted by mixing with other water masses. Similarly, Coniacian–Santonian black shales are recorded primarily from the Atlantic Ocean and the isotopic response to their deposition was greater in immediately adjacent areas. During the Campanian–Maastrichtian, however, it is suggested that water masses could exchange relatively easily between India and the northern margin of Africa and the Middle East, where black shales and phosphorites were deposited. (**b**) Tectonic map of Tibet, showing the location of the Tingri section and other localities referred to in the text. The Tethys Himalayas are divided into a southern subzone (A) and a northern subzone (B).

& Zhang 1993; Willems *et al*. 1996), but the positions of the stage boundaries were not accurately resolved. Consequently, we undertook a detailed biostratigraphic study before commencing the isotopic analyses. Determination of key microfossils allowed us to recognize a number of planktonic foraminiferal zones in the 270 m thick section. From base to the top, they are *R. reicheli*, *R. cushmani*, *W. archaeocretacea*, *H. helvetica*, *M. sigali*, *D. primitiva*, *D. concavata*, *D. asymetrica*, *G. elevata* and *G. ventricosa*. However, the absence of certain key Alpine–Mediterranean species in the higher part of the Tibetan succession (e.g. *G. calcarata*) renders difficult direct comparison with well-studied sequences, such as those exposed in the Italian Apennines (e.g. Premoli Silva & Sliter 1994). In this context, aided only by biostratigraphic data, the Campanian–Maastrichtian boundary presents particular difficulties. The first occurrence of *G. falsostuarti* (at 228.6 m at Gongzha), which has in the past been taken to define the latter stage boundary, is now known to occur in the *G. ventricosa* Zone of some researchers, both in the Italian Apennines and in the newly designated stage-boundary type section at Tercis les Bains, Landes, France (Ion & Odin 2001; Odin *et al*. 2001).

As regards the other boundaries, we place the Turonian–Coniacian contact in the interval 87.05–87.35 m and the Santonian–Campanian boundary in the interval 161.65–161.90 m, based on the first occurrences of diagnostic species (*D. primitiva and G. elevata*, respectively). The Coniacian–Santonian stage boundary we tentatively place at 135 m in the uppermost part of the *D. concavata* zone, in line with other low-latitude zonation schemes (Sliter 1989; Premoli Silva & Sliter 1994). Because the standard zonal nannofossils and ammonites are not present close to the Cenomanian–Turonian boundary in the section we place this level at 62.4 m in the upper *W. archaeocretacea* zone, according to the characteristic shape of the carbon-isotope curve (see Tsikos *et al*. 2004). Based on carbon-isotope curves from Europe and North Africa that illustrate a well-defined negative excursion at the top of the Campanian (Jenkyns *et al*. 1994; Jarvis *et al*. 2002), the boundary with the Maastrichtian must lie close to the top of the measured section and is tentatively located at *c*. 255 m by comparison with these reference sections (Fig. 2).

The lithology of the Upper Cretaceous cropping out at the Gongzha section of Tingri is dominated by fine-grained hemipelagic calcareous mudstones containing minor quartz silt, inter-

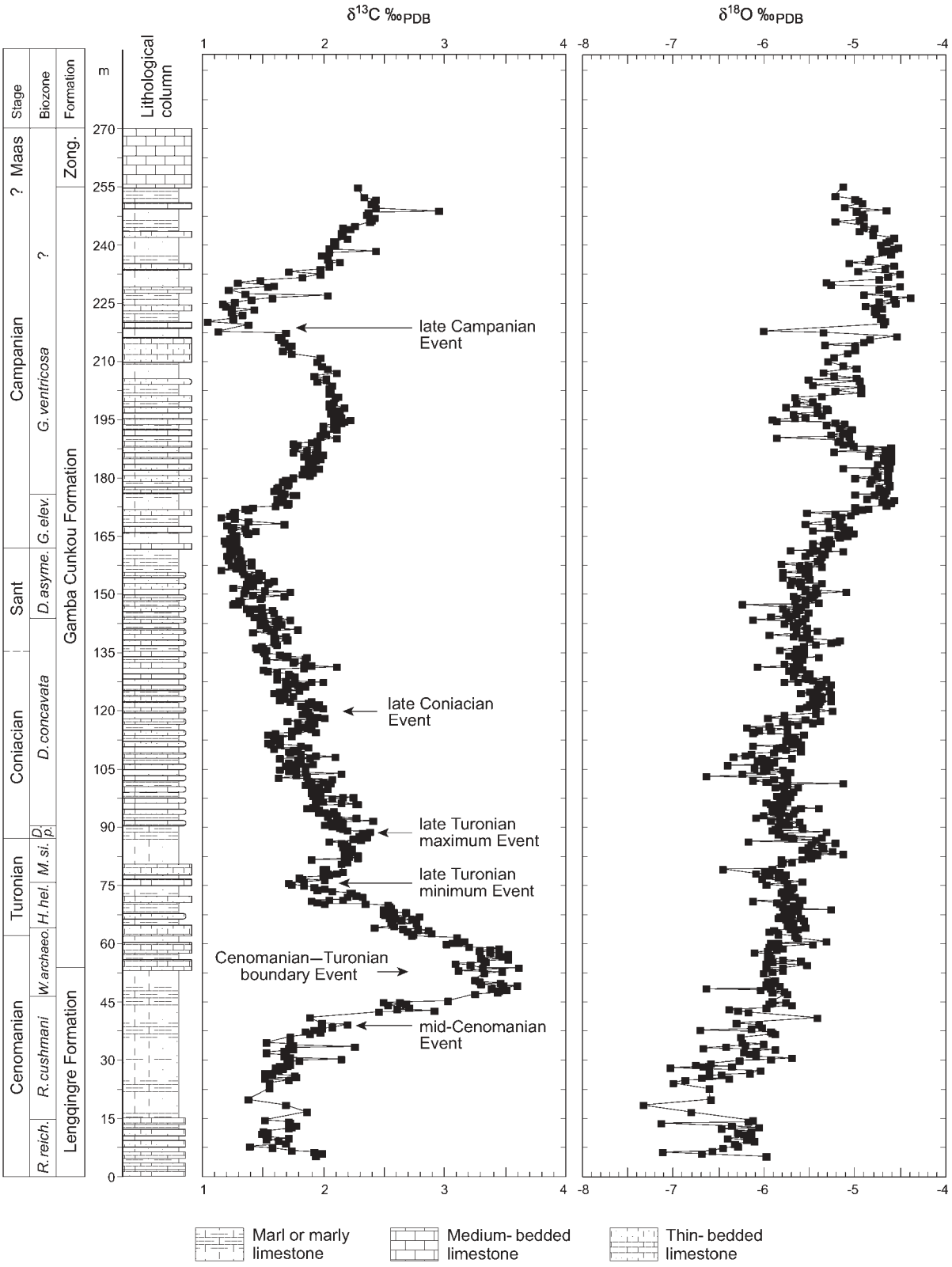

Fig. 2. Formations and lithologies exposed at Tingri with suggested biostratigraphic framework based on planktonic Foraminifera and accompanying isotope stratigraphy. The distinctive positive carbon-isotope excursion covering the Cenomanian–Turonian boundary and the less pronounced but well-defined positive carbon-isotope excursion in the middle Campanian should be noted. Lower-amplitude $\delta^{13}C$ positive excursions are centred at the Turonian–Coniacian boundary and the upper Coniacian. There is a pronounced negative $\delta^{13}C$ excursion in the upper Campanian. The oxygen-isotope profile shows an irregular but systematic drift to progressively higher values from the base to the top of the section.

preted as having been deposited in an open-marine basin and slope setting. Characteristic biota of the sediments in this area includes planktonic and benthonic Foraminifera, calcispheres, thin-shelled bivalves and some ammonites, all of whose skeletal cavities, where present, are locally occluded by sparry calcite (Willems *et al*. 1996). The Lengqingre Formation is mainly composed of grey marly mudstones with a few interbeds of marlstone and limestone; these pass into somewhat thicker-bedded marlstones, with intercalated limestones of the lower part of the Gamba Cunkou Formation. These sediments in turn pass up into grey centimetre-scale cycles of marly mudstone and marlstone that weather to a whitish colour. The cyclic depositional theme continues into the upper part of the Gamba Cunkou Formation (Fig. 2). The overlying Zongshan Formation is dominated by light grey medium- and thick-bedded limestones with a few interbedded units of calcareous mudstone. Larger benthic Foraminifera, probably redeposited, appear in the uppermost metre of the section (270 m).

The outcrop west of Tingri shows a general resemblance to the better-documented Gamba Zongshan section, situated some 200 km to the east (Wan *et al*. 2000; Zhao 2001). Lithofacies and microfacies of the Upper Cretaceous in both the Gamba and Tingri sections have been described in detail by Willems (1993), Willems & Zhang (1993) and Willems *et al*. (1996).

Materials and methods

Wherever possible lithological samples were collected at a 30–40 cm interval: 200 samples in 82 m of upper Cenomanian and Turonian sediment and 416 samples in 170 m of Coniacian–lower Maastrichtian sediment. Small amounts of powder were scratched from each sample and homogenized. Whole-rock carbon- and oxygen-isotope analyses were performed in the Department of Earth Sciences at the University of Oxford, UK. Samples were cleaned using 10% H_2O_2 followed by acetone and then dried at 60 °C. They were subsequently reacted with purified orthophosphoric acid at 90 °C and analysed on-line using a VG Isocarb device and Prism mass spectrometer. Normal corrections were applied and the results are reported, using the usual δ notation, in per mil deviation from the PDB standard. Calibration to PDB was performed via our laboratory standard calibrated against NBS19 and Cambridge Carrara marble. Reproducibility of replicate analyses of standards was generally better than 0.1‰ for both carbon- and oxygen-isotope ratios.

Results

A cross-plot of carbon- and oxygen-isotope values shows no significant trends and lacks the pronounced slope seen in many so-called 'mixing lines' produced by the addition of variable quantities of isotopically homogeneous cement to isotopically homogeneous skeletal calcite: most $\delta^{18}O$ values fall in the range −6.5 to −4.5‰; most $\delta^{13}C$ values fall in the range 1–3.5‰ (Fig. 3). The relatively low oxygen-isotope ratios, which depart from typical values found in poorly consolidated Cretaceous pelagic sediment (see Jenkyns *et al*. 1994; Clarke & Jenkyns 1999), must imply a considerable diagenetic overprint. Indeed, the overall pattern of increasingly lower $\delta^{18}O$ values with depth is consistent with temperature- and pressure-related burial diagenesis. These effects may be magnified by the known propensity of the oxygen in carbonates to exchange readily with the oxygen in pore waters, a phenomenon that does not similarly affect carbon because of its relative scarcity in interstitial fluids (Scholle & Arthur 1980). However, the relative coherence of the $\delta^{18}O$ stratigraphic plot (Fig. 2) is also compatible with the preservation of a primary trend, implying that recrystallization and/or the addition of diagenetic calcite (the effect of which is

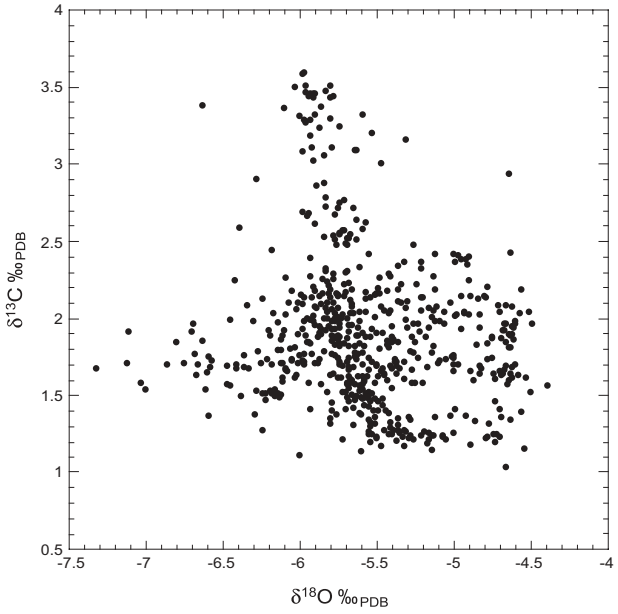

Fig. 3. Cross-plot of carbon- and oxygen-isotope ratios for bulk samples analysed from the Cretaceous hemipelagic section at Tingri. There is no significant correlation between the two sets of values. Both carbon- and oxygen-isotope values are consistently lower than those from chalks and pelagic limestones in Europe.

illustrated by the presence of sparite fills in some microfossils) has taken place in such a way that the ratio of primary to secondary calcite is roughly constant throughout the section and that carbonate cement was locally derived. Given that the pattern of $\delta^{13}C$ values generally conforms to global trends, the characteristic form of this curve is deemed to reflect primary seawater values with any diagenetic effects similarly affecting the section in a generally consistent manner (Scholle & Arthur 1980; Jenkyns *et al*. 1994).

The most obvious feature seen in the carbon-isotope profile is the pronounced positive excursion characteristic of the upper Cenomanian and the lowermost Turonian (principally *Whiteinella archaeocretacea* Zone) where $\delta^{13}C$ values rise to 3.5‰ from a background of *c*. 1.5‰. The detailed plot (Fig. 4) shows the excursion to be characterized by a broad plateau, as seen in many stratigraphic sections that are expanded enough to reveal exact structure (e.g. Paul *et al*. 1999; Tsikos *et al*. 2004). The curve also contains some small subsidiary peaks (*c*. 0.5‰ positive shift) in the lower Turonian, above which values fall back to a relative minimum of *c*. 1.5‰ before rising to a relative maximum of *c*. 2.3‰ at the boundary with the Coniacian (Fig. 2). This relative minimum, and the ensuing upper Turonian relative maximum, would appear to correspond to similar features seen in the lower part of the upper Turonian in the English Chalk and other pelagic-carbonate sections in Germany, Italy and Spain (see Jenkyns *et al*. 1994; Voigt & Hilbrecht 1997; Wiese 1999; Stoll & Schrag 2000; Voigt 2000). A subdued broad positive excursion in the middle Coniacian, very weakly developed compared with those in European carbon-isotope profiles (see Jenkyns *et al*. 1994; Stoll & Schrag 2000) interrupts a general fall in values from the base of the stage (*c*. 2‰) to the lower Campanian (*c*. 1‰): this overall downward trend contrasts with that seen in European sections. The bulk of the Campanian is defined by a broad positive excursion whose acme (*c*. 2‰) is at

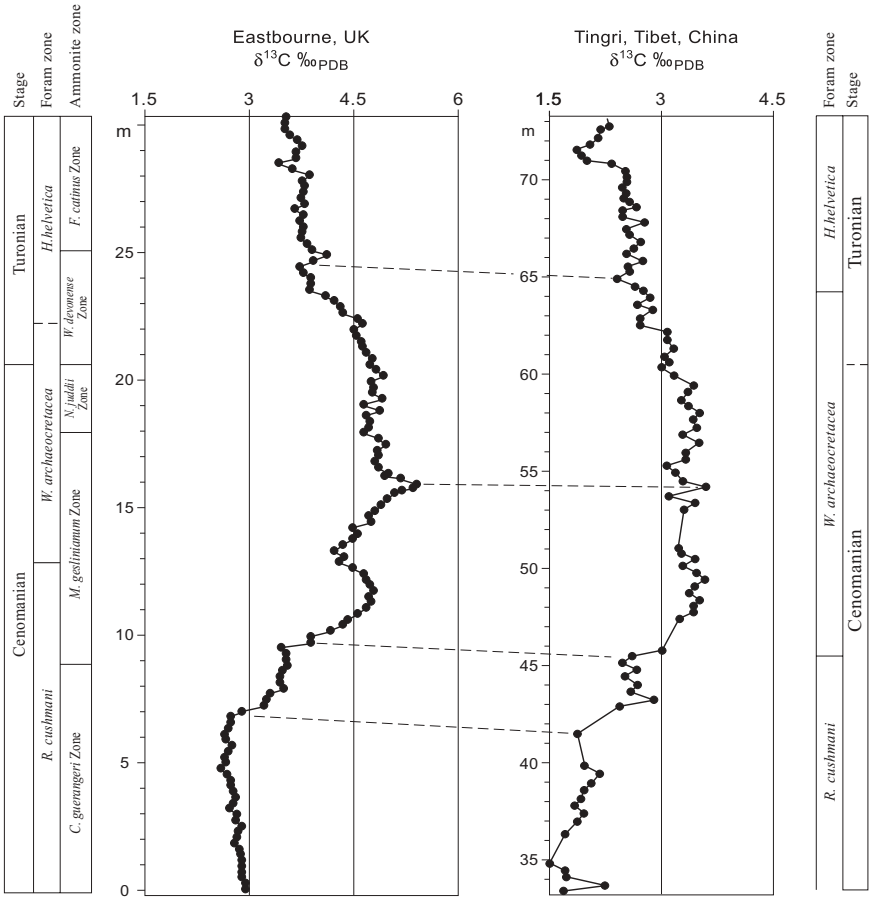

Fig. 4. Detailed comparison of the carbon-isotope evolution of the Cenomanian–Turonian boundary interval in Tingri, Tibet and Eastbourne, southern England. Although the Tibetan section shows $\delta^{13}C$ values that are systematically lower than those of Eastbourne by *c*. 1.5‰, the respective shapes of the positive excursion are remarkable similar to one another. Dashed lines indicate probably correlative levels, based on the chemostratigraphic curves. Eastbourne biostratigraphy and isotope stratigraphy are from Tsikos *et al*. (2004) and Gale *et al*. (2005), with additional foraminiferal data from Keller *et al*. (2001).

the mid-point of the stage (Fig. 5). From a minimum in the uppermost Campanian (*c*. 1‰), following a pronounced negative excursion, $\delta^{13}C$ values climb towards the lower Maastrichtian. European sections show a small positive excursion, rising to between 2 and 3‰, at the very base of the Campanian following which, in sections and cores through the English Chalk, there is a drop of *c*. 0.5‰ followed by a gradual rise to 2.5‰ in the middle of the stage (Jenkyns *et al*. 1994). A negative excursion in the higher Campanian, well developed in the English Chalk, can be correlated with a similar feature that delineates the end of the positive excursion in the Tibetan section (Fig. 5): this is certainly a global feature that has also been recorded from Ocean Drilling Program Site 869 off the Marshall Islands in the North Pacific (Jenkyns *et al*. 1995). This pronounced feature, named the Late Campanian Event, is also reproduced in sections from southern France and Tunisia (Clauser 1994; Jarvis *et al*. 2002) and has excellent potential as an inter-continental correlative tool. The middle Campanian $\delta^{13}C$ profile from North Africa most closely resembles that from Tibet.

The oxygen-isotope curve (Fig. 2) shows a general movement to higher values through the section, beginning with $\delta^{18}O$ values between −7 and −6‰ $\delta^{13}C$ in the middle Cenomanian and finishing with values *c*. −5‰ around the Campanian–Maastrichtian boundary. However, relatively coherent shifts towards higher values occur in the upper Turonian, middle Coniacian and lower Campanian. Relatively coherent shifts towards lower values occur in the middle Turonian, the lower Coniacian and the middle Campanian. Given that there is oxygen-isotope evidence, based on diagenetically immature sediments, for global climatic decline from Turonian time onward (Jenkyns *et al*. 1994; Clarke & Jenkyns 1999), the overall pattern seen in Tibet may record, to some degree, a decrease in water temperature. However, the particularly low background values suggest that original $\delta^{18}O$ values have been overprinted during burial-related recrystallization. Whether the $\delta^{18}O$ excursions relate to climatic perturbations or lithology-dependent diagenetic effects is unclear: they are not readily matched with oxygen-isotope profiles from elsewhere and hence are of unconstrained palaeoenvironmental significance.

Discussion and conclusions

Although the Tibetan carbon- and oxygen-isotope curves show a general similarity to those from Europe there are some significant differences. With reference to the carbon-isotope profile, the well-documented positive excursion at the Cenomanian–Turonian boundary is particularly well developed in Tibet. Indeed, the comparison with the carbon-isotope stratigraphy from Eastbourne is striking, even though the absolute values from the Tingri section are consistently less (by about 1.5‰) than those from the English Chalk (Fig. 4). Clearly, the accelerated burial of marine organic carbon in a range of environments across the globe during the Cenomanian–Turonian Oceanic Anoxic Event influenced water masses throughout the world ocean (Scholle & Arthur 1980.). Available data suggest that the most important locus of organic-carbon burial during the Cenomanian–Turonian

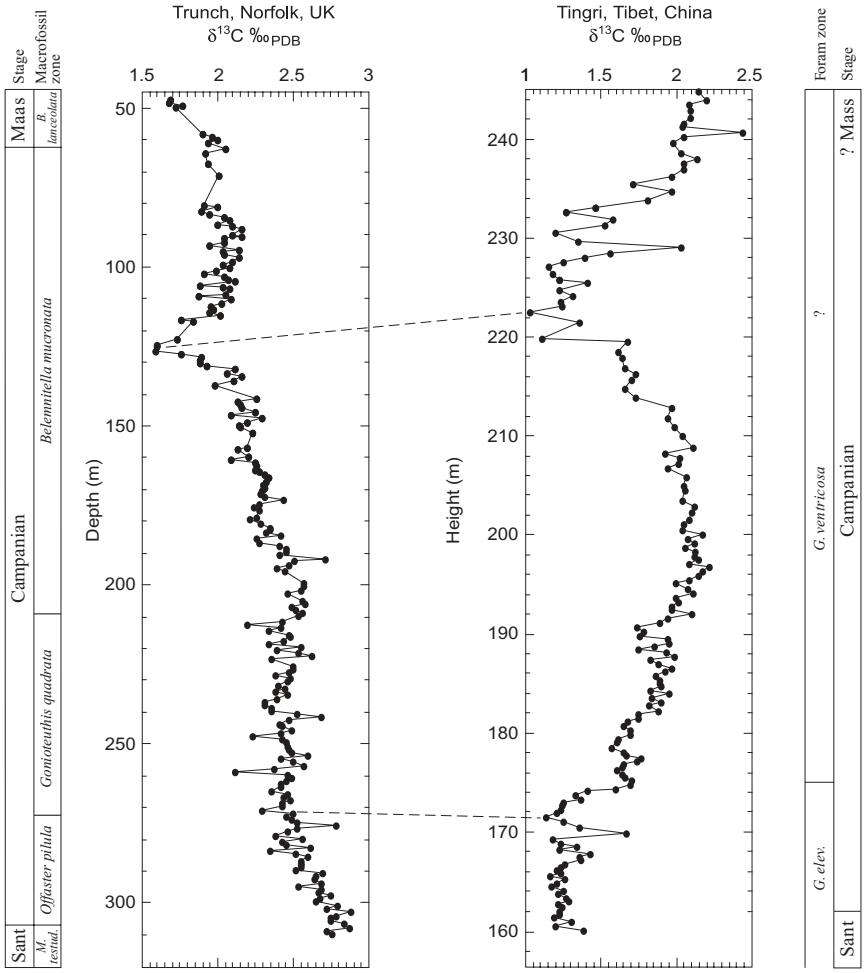

Fig. 5. Detailed comparison of the carbon-isotope evolution of the Campanian stage in Tingri, Tibet and the Trunch Borehole, southern England. Carbon-isotope values are similar in the two sections, but the positive excursion is much more pronounced in the Tibetan profile. Dashed lines indicate probably correlative levels, based on the chemostratigraphic curves. Trunch isotope data from Jenkyns *et al*. (1994).

Oceanic Anoxic Event was in the Atlantic–Caribbean–Tethyan region, where upwelling and elevated organic productivity was particularly important and euxinic conditions existed throughout much of the water column at certain times (Fig. 1; Schlanger *et al*. 1987; Sinninghe Damsté & Köster 1998; Kuypers *et al*. 2002; Pancost *et al*. 2004). In line with the view that waters potentially carrying the most positive $\delta^{13}C$ signature originated in the major organic-carbon sink of the peri-Atlantic region is the observation that the thickness and richness of organic-rich strata in North Africa decreases from west to east (Lüning *et al*. 2004). In Tibet itself total organic-carbon values of Cenomanian–Turonian marine facies are relatively low, only rarely exceeding 1% (Wang *et al*. 2001; Zou *et al*. 2005). The carbon-isotope signal in water masses influencing Tibet was hence more dampened than that in Europe.

The broad Coniacian shift to higher values to form a broad plateau extending into the Santonian (late Coniacian Event), well seen in sections from England and Italy, is rather poorly shown in Tibet and punctuates an overall decline in values (Fig. 2; see Jenkyns *et al*. 1994; Stoll & Schrag 2000). Black shales and mudstones of Coniacian–Santonian age are primarily developed in the Atlantic (particularly South Atlantic) and Caribbean regions (e.g. Ryan & Cita 1977; Wagner *et al*. 2004; Beckman *et al*. 2005) with relative organic-carbon enrichment (total organic carbon *c*. 10–20%) concentrated in the middle Coniacian to lower Santonian interval. It seems therefore that the shelf and marginal seas surrounding this zone of maximum organic-carbon burial experienced the consequent positive carbon-isotope excursion more intensely than did other oceans, where mixing of water masses diluted the isotopic signal. With regard to the Campanian positive $\delta^{13}C$ excursion (Fig. 5), the reverse is the case: the excursion is more conspicuous in the Tibetan section than in Europe, even though absolute peak-excursion values are not dissimilar (*c*. 2–2.5‰) in both cases. The middle Campanian positive excursion, and particularly its relative amplification in the Tibetan section, may relate to the large-scale deposition of organic-rich limestones, shales, cherts and phosphorites along the northern margin of Gondwana, well documented from a zone stretching between North Africa and the Middle East (e.g. Ganz *et al*. 1990; Robison & Engel 1993; Robison 1994); this sink for organic carbon could have produced water masses that could readily exchange with the Tibetan area during the Cretaceous (Fig. 1). The particular similarity between Campanian carbon-isotope curves from Tibet and Tunisia is consistent with this interpretation. The highest organic productivity in parts of Israel, as interpreted from palaeontological indices as well as the presence of organic matter, is dated to the late Campanian (Almogi-Labin *et al*. 1993), conforming exactly to the age of the positive carbon-isotope excursion.

However, the cause of the subsequent negative shift that terminates the middle Campanian carbon-isotope maximum remains problematic. This negative shift, with a clearly stepped profile in curves from both from the English Chalk and the hemipelagic marls from Tibet (Figs 2 and 5), must have been

caused by introduction of isotopically light carbon into the ocean–atmosphere system, perhaps from dissociation of gas hydrates and/or oxidation of organic matter on shelves affected by marine regression (Jarvis *et al*. 2002). Stepped excursions are a feature of those abrupt falls in $\delta^{13}C$ values attributed to dissociation of gas hydrates (Jenkyns 2003), but, although the data are suggestive, the sampling resolution of both the Tibetan and English sections is not high enough to decide whether or not there is a coherent oxygen-isotope shift to lower values at the same stratigraphic level that might imply coincident rapid global warming. Deposition of black shales and brown limestones on the northern margin of Gondwana continued well into the Maastrichtian, implying that any mechanism behind the negative carbon-isotope excursion would have had to counteract a tendency towards relatively high $\delta^{13}C$ values in adjacent seaways and oceans resulting from sequestration of organic carbon.

As far as inter-continental stratigraphic correlation is concerned, some segments of the high-resolution carbon-isotope curve from Tibet can be readily matched with those from biostratigraphically well-calibrated sections in Europe, although others are more problematic. None the less, carbon-isotope curves continue to offer considerable refinement of stratigraphy based purely on planktonic Foraminifera. In this context, the abrupt negative excursion high in the Campanian (late Campanian Event) now seems particularly valuable as a stratigraphic marker for those parts of the globe that lack key index species and where the boundary with the Maastrichtian stage is problematic.

This work was financially supported by the NSFC 40273014, the key NSFC 40332020 and National Basic Research Programme of China (973): 2006CB701401. H. Shi and P. Zhao analysed and identified the planktonic foraminifers. W. Kuhnt and X. Wan gave advice on identification of standard zonal species and age assignment. L. Jansa assisted in some of the fieldwork. Thanks are due to N. Charnley for help in the isotope laboratory in Oxford and to I. Jarvis for a very helpful review.

References

Almogi-Labin, A., Bein, A. & Sass, E. 1993. Late Cretaceous upwelling system along the southern Tethys margin (Israel): interrelationship between productivity, bottom water environments, and organic matter preservation. *Paleoceanography*, **8**, 671–690.

Arthur, M.A., Schlanger, S.O. & Jenkyns, H.C. 1987. The Cenomanian–Turonian oceanic anoxic event II, Palaeoceanographic controls on organic-matter production and preservation. *In:* Brooks, J. & Fleet, A.J. (eds) *Marine Petroleum Source Rocks*. Geological Society, London, Special Publications, **26**, 401–420.

Arthur, M.A., Dean, W.E. & Pratt, L.M. 1988. Geochemical and climatic effects of increased marine organic carbon burial at the Cenomanian/Turonian boundary. *Nature*, **335**, 714–717.

Arthur, M.A., Jenkyns, H.C., Brumsack, H.J. & Schlanger, S.O. 1990. Stratigraphy, geochemistry and paleoceanography of organic carbon-rich Cretaceous sequences. *In:* Ginsburg, R.N. & Beaudoin, B. (eds) *Cretaceous Resources, Events and Rhythms*. NATO ASI Series C, **304**, 75–119.

Beckman, B., Wagner, T. & Hofmann, P. 2005. Linking Coniacian–Santonian (OAE3) black shale formation to African climate variability: a reference section from the eastern tropical Atlantic at orbital time scales (ODP Site 959, off Ivory Coast/Ghana. *In:* Harris, N.B. & Pradier, B. (eds) *Organic Carbon-rich Sediments: Models, Mechanisms and Consequences*. Society for Sedimentary Geology (SEPM), Special Publications, **82**, 125–143.

Boersma, A. & Shackleton, N.J. 1981. Oxygen- and carbon-isotope variations and planktonic-foraminifer depth habitats, Late Cretaceous to Paleocene, central Pacific, Deep Sea Drilling Project Sites 463 and 465. *In:* Thiede, J. & Vallier, T. *et al. Initial Reports of the Deep Sea Drilling Project*, **62**. US Government Printing Office, Washington, DC, 513–528.

Bowman, A.R. & Bralower, T.J. 2005. Paleoceanographic significance of high-resolution carbon isotope records across the Cenomanian–Turonian boundary in the Western Interior and New Jersey coastal plain, USA. *Marine Geology*, **217**, 305–321.

Clarke, L.J. & Jenkyns, H.C. 1999. New oxygen-isotope evidence for long-term Cretaceous climatic change in the Southern Hemisphere. *Geology*, **27**, 699–702.

Clauser, S. 1994. *Études stratigraphiques du Campanien et du Maastrichtien de l'Europe occidentale: Côte Basque, Charentes (France), Limbourg (Pays-Bas)*. Documents du BRGM, **235**.

Dickens, G.R., O'Neil, J.R., Rea, D.C. & Owen, R.M. 1995. Dissociation of oceanic methane hydrate as a cause of the carbon isotope excursion at the end of the Paleocene. *Paleoceanography*, **10**, 965–971.

Erbacher, J., Friedrich, O., Wilson, P.A., Birch, H. & Mutterlose, J. 2005. Stable organic carbon isotope stratigraphy across Oceanic Anoxic Event 2 of Demerara Rise, western tropical Atlantic. *Geochemistry, Geophysics, Geosystems*, **6**, doi:10.1029/2004GC000850.

Gale, A.S., Jenkyns, H.C., Kennedy, W.J. & Corfield, R.M. 1993. Chemostratigraphy versus biostratigraphy: data from around the Cenomanian/Turonian boundary. *Journal of the Geological Society, London*, **150**, 29–32.

Gale, A.S., Kennedy, W.J., Voigt, S. & Walaszczyk, I. 2005. Stratigraphy of the Upper Cenomanian–Lower Turonian Chalk succession at Eastbourne, Sussex, UK: ammonites, inoceramid bivalves and stable carbon isotopes. *Cretaceous Research*, **26**, 480–487.

Gansser, A. 1964. *The Geology of Himalayas*. Wiley, New York.

Gansser, A. 1991. Facts and theories on the Himalayas. *Ecologae Geologicae Helvetiae*, **84**, 33–60.

Ganz, H.H., Luger, P., Schrank, E., Brooks, P.W. & Fowler, M.G. 1990. Facial evolution of Late Cretaceous black shales from Southeast Egypt. *In:* Klitzsch, E. & Schrank, E. (eds) *Research in Sudan, Somalia, Egypt and Kenya: Results of the Special Research Project 'Geoscientific Problems in Arid and Semiarid Areas'*. Berliner Geowissenschaftliche Abhandlungen, Reihe A: Geologie und Paläontologie, **120**, 993–1010.

Hao, Y. & Wan, X. 1985. Marine Cretaceous and Tertiary in Tingri, Tibet. *Geological Contributions to Qinghai–Xizang Plateau*, **17**, 227–232 (in Chinese with English abstract).

Hasegawa, T. 1997. Cenomanian–Turonian carbon isotope events recorded in terrestrial organic matter from northern Japan. *Palaeogeography, Palaeoclimatogy, Palaeoecology*, **130**, 251–273.

Hasegawa, T., Pratt, L.M., Maeda, H., Shigeta, Y., Okamoto, T., Kase, T. & Uemura, K. 2003. Upper Cretaceous stable carbon isotope stratigraphy of terrestrial organic matter from Sakhalin, Russian Far East: a proxy for the isotopic composition of paleoatmospheric CO_2. *Palaeogeography, Palaeoclimatogy, Palaeoecology*, **189**, 97–115.

Hu, X., Wang, C. & Li, X. 2001. A relationship between stable carbon isotope and dissolved oxygen of Cretaceous marine carbonates in southern Tibet. *Progresses in Natural Sciences*, **11**, 721–728 (in Chinese).

Huber, B.T., Hodell, D.A. & Hamilton, C.P. 1995. Middle–Late Cretaceous climate of the southern high latitudes: stable isotopic evidence for minimal equator-to-pole thermal gradients. *Geological Society of America Bulletin*, **107**, 1164–1191.

Huber, B.T., Norris, R.D. & MacLeod, K.G. 2002. Deep-sea paleotemperature record of extreme warmth during the Cretaceous. *Geology*, **30**, 123–126.

Ion, J. & Odin, G.S. 2001. Planktonic Foraminifera from the Campanian–Maastrichtian at Tercis les Bains (Landes, France). *In:* Odin, G.S. (ed.) *The Campanian–Maastrichtian Stage Boundary*. Developments in Palaeontology and Stratigraphy, **19**, 349–378.

Jahren, A.H., Arens, N.C., Sarmiento, G., Guerrero, J. & Amundson, R. 2001. Terrestrial record of methane hydrate dissociation in the Early Cretaceous. *Geology*, **29**, 159–162.

Jarvis, I., Mabrouk, A., Moody, R. & de Cabrera, S. 2002. Late Cretaceous (Campanian) carbon isotope events, sea-level change and correlation of the Tethyan and Boreal realms. *Palaeogeography, Palaeoclimatology, Palaeoecology*, **188**, 215–248.

Jenkyns, H.C. 1980. Cretaceous anoxic events: from continents to oceans. *Journal of the Geological Society, London*, **137**, 171–188.

Jenkyns, H.C. 2003. Evidence for rapid climate change in the Mesozoic–Palaeogene greenhouse world. *Philosophical Transactions of the Royal Society, Series A*, **361**, 1885–1916.

Jenkyns, H.C., Gale, A.S. & Corfield, R.M. 1994. Carbon-isotope and oxygen-isotope stratigraphy of the English Chalk and Italian Scaglia and its palaeoclimatic significance. *Geological Magazine*, **131**, 1–34.

Jenkyns, H.C., Mutterlose, J. & Sliter, W.V. 1995. Upper Cretaceous carbon- and oxygen-isotope stratigraphy of deep-water sediments from the north–central Pacific (Site 869, Flank of Pikinni-Wodejebato, Marshall Islands). *In:* Winterer, E.L., Sager, W.V. & Sinton, J.M. (eds) *Proceedings of the Ocean Drilling Program, Scientific Results,* **143**. College Station, TX, 105–108.

Keller, G., Han, Q., Adatte, T. & Burns, S.J. 2001. Palaeoenvironment of the Cenomanian–Turonian transition at Eastbourne, England. *Cretaceous Research*, **22**, 391–422.

Kuypers, M.M.M., Pancost, R.D., Nijenhuis, I.A. & Sinninghe Damsté, J.S. 2002. Enhanced productivity led to increased organic carbon burial in the

euxinic North Atlantic basin during the Cenomanian/Turonian oceanic anoxic event. *Paleoceanography*, **17**, 1–13.

Lüning, S., Kolonic, S., Belhadj, E.M., Belhadj, Z., Cota, L., Baric, G. & Wagner, T. 2004. Integrated depositional model for the Cenomanian–Turonian organic-rich strata in North Africa. *Earth-Science Reviews*, **64**, 51–117.

Odin, G.S., Arz, J.A., Caron, M., Ion, J. & Molina, E. 2001. Campanian–Maastrichtian planktonic foraminifera at Tercis les Bains (Landes, France); synthetic view and potential for global correlation. *In:* Odin, G.S. (ed.) *The Campanian–Maastrichtian Stage Boundary*. Developments in Palaeontology and Stratigraphy, **19**, 379–395.

Pancost, R.D., Crawford, N., Magness, S., Turner, A., Jenkyns, H.C. & Maxwell, J.R. 2004. Further evidence for the development of photic-zone euxinic conditions during Mesozoic oceanic anoxic events. *Journal of the Geological Society, London*, **161**, 353–364.

Paul, C.R.C., Lamolda, M.A., Mitchell, S.F., Vaziri, M.R., Gorostidi, A. & Marshall, J.D. 1999. The Cenomanian/Turonian boundary at Eastbourne (Sussex, UK): a proposed European reference section. *Palaeogeography, Palaeoclimatology, Palaeoecology*, **150**, 83–121.

Pratt, L.M. & Threlkeld, C.N. 1984. Stratigraphic significance of $^{13}C/^{12}C$ ratios in mid-Cretaceous rocks of the Western Interior, USA. *In:* Stott, D.F. & Glass, D.J. (eds) *The Mesozoic of Middle North America*. Canadian Society of Petroleum Geologists, Memoirs, **9**, 305–312.

Premoli Silva, I. & Sliter, W.V. 1994. Cretaceous planktonic foraminiferal biostratigraphy and evolutionary trends from the Bottaccione section, Gubbio, Italy. *Palaeontographica Italica*, **82**, 1–89.

Robison, V.D. 1994. Source rock characterization of the Late Cretaceous Brown Limestone of Egypt. *In:* Katz, B.J. (ed.) *Petroleum Source Rocks*. Springer, Berlin, 265–281.

Robison, V.D. & Engel, M.H. 1993. Characterization of the source horizons within the Late Cretaceous transgressive sequence of Egypt. *In:* Katz, B.J. & Pratt, L.M. (eds) *Source Rocks in a Sequence Stratigraphic Framework*. AAPG Studies in Geology, **37**, 101–117.

Ryan, W.B.F. & Cita, M.B. 1977. Ignorance concerning episodes of ocean-wide stagnation. *Marine Geology*, **23**, 197–215.

Schlanger, S.O. & Jenkyns, H.C. 1976. Cretaceous oceanic anoxic events: causes and consequences. *Geologie en Mijnbouw*, **55**, 179–184.

Schlanger, S.O., Arthur, M.A., Jenkyns, H.C. & Scholle, P.A. 1987. The Cenomanian–Turonian oceanic anoxic event, I. Stratigraphy and distribution of organic rich beds and the marine $\delta^{13}C$ excursion. *In:* Brooks, J. & Fleet, A.J. (eds) *Marine Petroleum Source Rocks*. Geological Society, London, Special Publications, **26**, 371–399.

Scholle, P.A. & Arthur, M.A. 1980. Carbon isotope fluctuations in Cretaceous pelagic limestones: potential stratigraphic and petroleum exploration tool. *AAPG Bulletin*, **64**, 67–87.

Sinninghe Damsté, J.S. & Köster, J. 1998. A euxinic southern North Atlantic Ocean during the Cenomanian–Turonian oceanic anoxic event. *Earth and Planetary Science Letters*, **158**, 165–173.

Sliter, W.V. 1989. Biostratigraphic zonation for Cretaceous planktonic foraminifers examined in thin section. *Journal of Foraminiferal Research*, **19**, 1–19.

Smith, A.G., Hurley, A.M. & Briden, J.C. 1981. *Phanerozoic Paleocontinental World Maps*. Cambridge University Press, Cambridge.

Stoll, H.M. & Schrag, D.P. 2000. High-resolution stable isotope records from the Upper Cretaceous rocks of Italy and Spain: glacial episodes in a greenhouse planet? *Geological Society of America Bulletin*, **112**, 308–319.

Tsikos, H., Jenkyns, H.C. & Walsworth-Bell, B. *et al.* 2004. Carbon-isotope stratigraphy recorded by the Cenomanian–Turonian Oceanic Anoxic Event: correlation and implications based on three key-localities. *Journal of the Geological Society, London*, **161**, 711–719.

Veizer, J., Ala, D. & Azmy, K. *et al.* 1999. $^{87}Sr/^{86}Sr$, $\delta^{13}C$ and $\delta^{18}O$ evolution of Phanerozoic seawater. *Chemical Geology*, **161**, 59–88.

Villamil, T. & Arango, C. 1998. Integrated stratigraphy of latest Cenomanian and early Turonian facies of Colombia. *In:* Pindell, J.L. & Drake, C. (eds) *Paleogeographic Evolution and Non-glacial Eustasy, Northern South America*. SEPM (Society for Sedimentary Geology) Special Publications, **58**, 129–159.

Voigt, S. 2000. Cenomanian–Turonian composite $\delta^{13}C$ curve for Western and Central Europe: the role of organic and inorganic carbon fluxes. *Palaeogeography, Palaeoclimatology, Palaeoecology*, **160**, 91–104.

Voigt, S. & Hilbrecht, H. 1997. Late Cretaceous carbon isotope stratigraphy in Europe: correlation and relations with sea level and sediment stability. *Palaeogeography, Palaeoclimatology, Palaeoecology*, **134**, 39–59.

Wagner, T., Sinninghe Damsté, J.S., Hofmann, P. & Beckmann, B. 2004. Euxinia and primary production in Late Cretaceous eastern equatorial Atlantic surface waters fostered orbitally driven formation of marine black shales. *Paleoceanography*, **19**(PA3009), doi:10.1029/2003PA000898.

Wan, X., Zhao, W. & Li, G. 2000. Restudy of the Upper Cretaceous in Gamba, Tibet. *Geosciences*, **14**, 281–285 (in Chinese with English abstract).

Wan, X., Wei, M. & Li, G. 2003a. $\delta^{13}C$ values from the Cenomanian–Turonian passage beds of southern Tibet. *Journal of Asian Earth Sciences*, **21**, 861–866.

Wan, X., Wignall, P.B. & Zhao, W. 2003b. The Cenomanian–Turonian extinction and oceanic anoxic event: evidence from southern Tibet. *Palaeogeography, Palaeoclimatology, Palaeoecology*, **199**, 283–298.

Wang, C., Xia, D. & Zhou, X. *et al.* 1996. *Field Trip Guide: T121/T387 Geology between the Indus–Yarlung Zangbo Suture Zone and the Himalaya Mountains (Xizang), China*. Geological Publishing House, Beijing.

Wang, C.S., Hu, X.M., Jansa, L., Wan, X.Q. & Tao, R. 2001. The Cenomanian–Turonian anoxic event in southern Tibet. *Cretaceous Research*, **22**, 481–490.

Weissert, H. 1989. Carbon isotope stratigraphy, a monitor of palaeoenvironmental change: a case study from the early Cretaceous. *Surveys in Geophysics*, **10**, 1–61.

Weissert, H. & Erba, E. 2004. Volcanism, CO_2 and palaeoclimate: a Late Jurassic–Early Cretaceous carbon and oxygen isotope record. *Journal of the Geological Society, London*, **161**, 695–702.

Wiese, F. 1999. Stable isotope data ($\delta^{13}C$, $\delta^{18}O$) from the Middle and Upper Turonian of Liencres (Cantabria, northern Spain) and a comparison to northern Germany (Söhlde & Salzgitter-Salder). *Newsletters on Stratigraphy*, **37**, 37–62.

Willems, H. 1993. Sedimentary history of the Tibetan Tethys Himalaya continental shelf in South Tibet (Gamba, Tingri) during Upper Cretaceous and Lower Tertiary (Xizang Autonomous Region, PR China). *In:* Willems, H. (ed.) *Geoscientific Investigation in the Tethyan Himalayas*. Berichte aus dem Fachbereich Geowissenschaften der Universität Bremen, **38**, 49–183.

Willems, H. & Zhang, B. 1993. Cretaceous and Lower Tertiary sediments of the Tibetan Tethys Himalaya in the area of Tingri (South Tibet, PR China). *In:* Willems, H. (ed.) *Geoscientific Investigation in the Tethyan Himalayas*. Berichte aus dem Fachbereich Geowissenschaften der Universität Bremen, **38**, 28–47.

Willems, H., Zhou, Z., Zhang, B. & Gräfe, K.-U. 1996. Stratigraphy of the Upper Cretaceous and Lower Tertiary strata in the Tethyan Himalayas of Tibet (Tingri area, China). *Geologische Rundschau*, **85**, 723–754.

Zakharov, Y.D., Boriskina, N. & Ignatyev, A.V. 1999. Palaeotemperature curve for the Late Cretaceous of the northwestern circum-Pacific. *Cretaceous Research*, **20**, 685–697.

Zhao, W. 2001. Late Cretaceous foraminiferal faunas and eustatic change in Gamba Area, southern Tibet. *Geological Journal of China Universities*, **7**, 106–117 (in Chinese with English abstract).

Zou, Y.-R., Kong, F., Peng, P., Hu, X. & Wang, C. 2005. Organic geochemical characteristics of Upper Cretaceous oxic oceanic sediments in Tibet, China: a preliminary study. *Cretaceous Research*, **26**, 65–71.

Received 15 March 2005; revised typescript accepted 19 July 2005.
Scientific editing by Duncan McIlroy